Observatory Data: a 170-year Sun-Earth Connection

Leif Svalgaard

Introduction

The discovery of the sunspot cycle and the first results of the 'Magnetic Crusade' together made it clear that solar and geomagnetic activity are intimately related and that observing one is learning about the other [both ways]. Understanding of this magnificent relationship had to await more than a century of progress in both physics and observations, and only in the last few decades have we achieved the elucidation that in the middle of the 19th Century was so fervently hoped for: The lack of rapid progress so frustrated the observers [and their funding agencies] that many observatories were shut down or had operations severely curtailed, because as von Humboldt remarked in vol. 4 of his *Cosmos*: "they have yielded so little return in proportion to the labor that had gone into collecting the material". The confirmation by spacecraft measurements of what workers in solar-terrestrial relations had so long suspected namely that a solar wind connects the magnetic regimes of the Sun and the Earth has finally brought about an understanding of one half of the relationship [activity] while the discovery of the ionosphere and measurements of solar ultraviolet and X-ray emissions have brought understanding of the other half [regular diurnal variation]. We now have a quantitative understanding of these phenomena [although the microphysics is still debated] allowing us to model quantitatively the geomagnetic response to solar and interplanetary conditions. The immense complexity of geomagnetic variations becomes tractable by the introduction of suitable geomagnetic *indices* on a variety of time scales. Because different indices respond to different combinations of solar wind parameters we can invert the response and determine solar wind speed and density and interplanetary magnetic field strength from simple hourly mean values as far back as these are available, as we will show in this talk. In addition, the understanding of the ionospheric response to solar Far UltraViolet, allows us to infer FUV in the past as well, with the possibility of checking [and correcting] the sunspot number and calculating the Total Solar Irradiance. As geomagnetic variations have been monitored for ~170 years with [for this purpose] constant calibration, we have a data set of immense value for understanding long-term changes in the Sun. We argue that all efforts must be expended to preserve and digitize these national and scientific treasure troves.

The Central Problem of Geomagnetic Variations

The geomagnetic record shows a mixture of signatures from different physical processes: the regular daily variation, irregular short duration [1-3 hours] variations, and 'storms' typically lasting a day or more. Geomagnetic *indices* have been devised to characterize and quantify these three types [ignoring special effects like pulsations, eclipse effects, etc]. An experienced observer can usually distinguish the various types from the general character of the curves and from hers/his knowledge of the *typical* variations at the observatory. Various computer algorithms more or less successfully attempt to supplant the need for a human, experienced observer, but in any case, the *high-frequency* part of the record is the necessary ingredient in the process.

The Difficulty with the Regular Daily Variation

Recognizing and quantifying the regular daily variation, what Mayaud called S_R, is the main problem. The amplitude of this variation varies from day to day; near the focus of the current system, even the type of the variation changes from day to day. And at low latitudes the large summer vortex from the other hemisphere intrudes into the winter hemisphere. In deriving both the *Dst* index and the *K* range index, S_R must be recognized and removed. We all know the problems associated with that, with the insufficiency of using the'5 Quiet Days' as the basis for determining S_R, and with the error of using an average 'iron curve', etc. The pattern-recognition capabilities of the experienced observer cannot be transferred to successors.

Long-Term Geomagnetic Indices

Mayaud's heroic construction [1972] of the *aa-index* (back to 1868) is unlikely to be duplicated. The international cooperation and effort that are providing us with the *ap* (1932-), *am* (1959-), and *Dst* (1957-) indices cannot be replicated or extended into the past. It is difficult to gauge the long-term stability of the calibration of the range indices. The vast collection of 19th Century *yearbook* data seems useless to many people to the point where the data is not being preserved or digitized for modern processing methods. *In this talk, I'll show how these problems can be overcome and provide a rationale for the preservation and digitization of the yearbook data.*

***IHV*-index: Use of Night Hours Only**

Figure 1 shows the variation of the three geomagnetic components, H, D, and Z at FRD (Fredericksburg) during several days. The regular variation is clearly seen on every day including the day-to-day variation. Since the ionospheric conductivity is down by two orders of magnitude during local night, S_R is effectively absent during the night hours. So, the solution to the problem of elimination of S_R is simply to construct an index using only local night hours; by throwing away 75% of the data, you remove 99% of the problem. Red boxes outline the local night.

Svalgaard and Cliver [2004, 2007a] introduced a new index based on this approach. The *IHV*-index (InterHourly Variability) is defined as the sum of the *absolute values* of the six differences between hourly values of any of the geomagnetic components [initially for H] for the seven hours spanning local midnight (generally falling within the 4th hour). In practice, we determine the *number of hours to skip* from 0^h UT, before beginning to sum the following six hourly absolute differences. Local midnight is also the time where the correlation with interplanetary parameters maximizes. A most important detail is that *hourly mean values* are used, so that no high-resolution data is needed, and the vast store of *yearbook*-style data that exists can be brought to bear.

Correcting *IHV* from Hourly *Values* to the Level of Hourly *Means*

Starting in 1905 Adolf Schmidt at Potsdam began to use Hourly Means instead of the Hourly point Values that had traditionally been reported in yearbooks. And soon most observatories adopted the new practice. [Some waited long, e.g. the French, who held out to 1972, before making the switch]. The instantaneous values read once every hour have larger variance which results in larger *IHV*. This is easily corrected for, e.g. by calculating *IHV* from hourly means [from the 60 one-minute values] and from hourly point values and comparing the two *IHVs.* All early observatory data must be (and has been) so corrected.

IHV is Strongly Correlated With the *Am*-index

The best global activity index seems to the *am*-index [Mayaud, 1967] due to its excellent spatial coverage. There is a strong correlation (Figure 2) between *IHV* [blue] and the *am*-index [red]. For monthly means for FRD, we can calculate *am* from the regression equation $am_{calculated} = 0.7475\ IHV$. The calculated *am*-index [pink] is a good proxy for *am* over the same six-hour interval [00-06 UT] as was used in the calculation of *IHV*. Using several stations at different longitudes, a global composite *IHV* can now be constructed. The correlation with *am* is very high ($R^2 = 0.96$ for monthly or 27-day rotation means), which means that we can reconstruct the *am*-index as far back as we can get *IHV*.

Variation of *IHV* With Latitude

For *all* (~120) stations that had [essentially complete] data during 1996-2003, we calculated the average *IHV* for each station over that interval and plotted it against corrected geomagnetic latitude and found that *IHV* increases sharply in the auroral zones and we ***limit*** ourselves now to stations below 55° corrected geomagnetic latitude, for which the variation with latitude is very slight.

Semiannual Variation of (Raw) *IHV*

IHV exhibits the 'usual' equinoctial semiannual variation [e.g. Svalgaard et al., 2002, and references therein]. This variation is well described by the '*S*'-function of the Earth's dipole tilt, $\Psi(doy, UT)$, against the solar wind direction:

$$S(\Psi) = 1/(1 + 3\cos^2(\Psi))^{2/3} \quad (1)$$

We remove this purely terrestrial effect simply by dividing the raw *IHV* for each station by the *S*-function for that station at the day of year, 'doy', and UT time for every single *IHV* value. This makes it possible to combine records from stations at different longitudes regardless of data gaps. If desired the *S*-function can be applied in reverse to add the variation back in. The fact that *IHV* shows the semiannual (including its UT component) variation so well attests to its efficacy and accuracy as a measure of global geomagnetic activity.

Stations Used for Construction of *IHV*-index

As Figure 3 shows, we use 12 independent longitude [and North/South] "boxes" plus an Equatorial band [blue station symbols]. For each box, a *reference* station is shown in pink. *IHV* for all other stations in the box are normalized to the reference station and the average is computed for the box. Finally, each box is normalized to the European box [Reference station: Niemegk]. From now on we shall works with 27-day Bartels rotation averages for economy of presentation. The stations have been chosen for their long series of hourly mean values and the large number used makes *IHV* robust and rather insensitive to minor errors in the data.

Composite Global *IHV*-index

By averaging [with equal weight] all the normalized 'box' composites we arrive at a *global* composite *IHV*-index that covers all UT hours. Figure 4(a) shows several years of the individual box-series to illustrate the consistent response from box to box. Note that there is no clear seasonal difference between north [black] and south [red]. Using stations back to the First Polar Year in 1883 a composite *IHV*-index since then can be constructed. The result is shown in Figure 4(b) including a 13-rotation running mean. Arrows show years with strong high-speed streams.

Comparison with Amplitude (Range) Indices

We wish to compare the long series of composite *IHV* with the classical range indices, *am*, *ap*, and *aa*, in order to verify to what degree we have succeeded in producing a comparable index. Since *IHV* is freed from the semiannual variation we also divide the range indices by the S-function and then regress the Bartels rotation means against *IHV*. The relationships are slightly non-linear (most so for the *Ap*-index), but are all highly significant (coefficients of determination R^2 are in excess of 0.9). For the *Aa*-index we have chosen to regress over the time since 1980 where there has been no change in *aa*-stations (and, hopefully, neither in procedures or calibration).

We can now use these empirical regression equations [e.g. $Am = 0.2375\ IHV^{1.2892}$, $R^2 = 0.96$] to *calculate* the classical indices for comparison with *IHV*: The result is shown in Figure 5, where heavy lines show 13-rotation running means. As expected, the fit to *Am* is excellent, so *IHV* is, indeed, an excellent proxy for *Am*. For *Ap*, there are times when the fit is less good. We interpret those as indications of inhomogeneities in the *Ap*-index, and note that there is no systematic trend in the differences.

For *Aa*, the calculated values [$Aa = 0.36\ IHV^{1.1856}$, $R^2 = 0.95$] match well back to 1957, but before that time, the observed values of *Aa* fall consistently 3-4 nT below the values derived from *IHV*. A similar discrepancy has been reported by other groups [Jarvis, 2005; Mursula & Martini, 2006; Rouillard et al., 2007] and must now be considered as established. It would thus seem that the *aa*-index is in need of a recalibration.

Physical Meaning of *IHV* (and *am*, *aa*, *ap*)

Geomagnetic activity as given by the three-hour *am*-index has been found [Svalgaard 1978] to depend on solar wind parameters and the geometry of their interaction with the Earth as this:

$$am = k\,(nV^2)^{1/3}\,(BV)\,q(\alpha, f)\,S(\Psi) \qquad (2)$$

where the various factors have meaning of Momentum flux, Magnetic Reconnection, and Geometric Modulation, and where *B* is the Interplanetary Magnetic Field (IMF) strength, *V* is the Solar Wind Speed, *q* is a function of the angle α between the IMF and the Earth's magnetic field at the 'nose' of the magnetopause, and the relative variability *f* is defined as $\sqrt{(\sigma_{Bx}^2 + \sigma_{By}^2 + \sigma_{Bz}^2)}/\sigma_B$.

Figure 6 shows how good the fit is for individual three-hour intervals [red curves = calculated *am*; note the logarithmic-scale]. Only for very small values of *am* [<5 nT] where *am* is almost impossible to measure correctly do we have a persistent discrepancy: *am*, or rather *Km*, is too low. $K = 0$ is always a problem.

For intervals longer than three hours the variables are weakly correlated and the relation becomes slightly modified to $am \sim BV^2$. We would therefore expect a similar relationship for *IHV*. This is indeed what is observed: Figure 7(a). In Figure 7(b) we show a comparison of observed (red] and calculated values (black) of BV^2, using the regression equation of Figure 7(a). It is evident that *IHV* is good proxy for BV^2. It is somewhat remarkable that *am* [based on *K* indices conceived so long ago] also is.

During geomagnetic activity, magnetospheric particles are accelerated and precipitate into the upper atmosphere over the polar regions where the energy thus deposited can be directly measured by polar-orbiting satellites (POES). From the satellite data, the total energy input (in GigaWatt) to each hemisphere can be estimated. Such estimates exist back to 1978 [Emery et al., 2008].We find that *IHV* is directly proportional to the power input, *Hp*, to the upper atmosphere, *Hp* = 0.68 *IHV* GW.

The IDV-Index, a Modern Version of the *u*-measure

The *IHV*-index captures activity on a time scale of hours. How about on a time scale of days? Julius Bartels (building on work by Adolf Schmidt) defined the *u*-measure as the monthly (or yearly) mean of the unsigned differences between the mean values of the H-component on two successive days [Joos et al., 1952]. We found that you get essentially the same result using the mean over the whole day, a few hours, or only one hour. Our InterDiurnal Variability index [*IDV*, Svalgaard & Cliver, 2005] is then simply the average *u*-measure (in nT, not the original 10 nT units) using only one hour (preferably the midnight hour if available) for as many stations as possible below 51° corrected geomagnetic latitude: Figure 8 shows yearly averages of the *u*-measure and *IDV*. During their time of overlap, the match is excellent.

Note that *u* and *IDV* did not register the strong high-speed streams in 1910, 1930, 1952, 1974, 1994, and 2003. This (especially for 1930) was a deadly blow to the *u*-measure, and Bartels effectively dropped the index and went on to invent his much more successful *K*-index.

What is the *IDV*-index Measuring? IMF Strength !

IDV does not ‘see’ the high-speed solar wind. But there is a robust correlation with the IMF magnitude, *B*; see Figure 9(a). This is shown more explicitly on an event-by-event basis in Figure 9(b). So instead of the *u*-measure being a ‘failure’, its modern equivalent [*IDV*] and thus the *u*-measure itself have a very useful property: response to *B* only.

Coronal Mass Ejections (CMEs) add (closed) magnetic flux to the IMF. CMEs hitting the Earth create magnetic storms feeding energy into the inner magnetosphere (“ring current”). The *Dst*-index is aimed at describing this same phenomenon, but only the negative contribution to *Dst* on the nightside is effectively involved. We therefore expect (negative) *Dst* and *IDV* to be strongly related, and they are [R^2 = 0.89 for yearly averages]. We used a new derivation of *Dst* by J. Love back to 1905 [Love, 2007]. Similar results are obtained with the *Dst* series by Karinen & Mursula [2005] (to 1932) or with the “official” *Dst* series (to 1957). The very simple-to-derive *IDV* series compares favorably with the much more elaborate *Dst*(< 0). Using regressions of *IDV* and *Dst* (< 0) on IMF *B* we can directly estimate *B* back to 1872 [Figure 11(a)].

Since there is also a good correlation between *B* and the square root of the sunspot number, *Rz*, [Svalgaard et al., 2003; Karinen & Mursula, 2006], we can infer *B* from *Rz* as well. Can we go further back in time? Schmidt and Bartels had determined the *u*-

measure from 1836 on, but with less confidence before 1872. We thus have a measure of *u* and therefore of *IDV* (and then inferentially *B*) back to 1836:

Polar Cap Current and Polar Cap Potential

Across the Earth's polar caps flows a current in the ionosphere. This is a Hall current basically flowing towards the sun. The Earth rotates under this current causing the magnetic effect of the current to rotate once in 24 hours. This rotating daily effect is readily (and has been since 1883, Figure 10(b)) observed as a circle in the X and Y component coordinates at polar cap magnetic observatories. The current derives from the Polar Cap Electric Potential which is basically the electric field ($\boldsymbol{E} = -\boldsymbol{V}\text{x}\boldsymbol{B}$) in the solar wind mapped down to the ionosphere. The radius of the circle traced out by variation of horizontal components is a measure of the polar cap potential [Figure 10(a)] and is essentially the same for all stations within the polar cap. For stations near the polar cap boundary, the circle is only partial and persists only when the station is inside the polar cap. From the size of the circle during the spacecraft area we can calibrate the variation in terms of the product *VB* [Le Sager & Svalgaard, 2004].

An Over-determined System

We now have three independent ways of estimating solar wind and IMF parameters:

1. The *IHV*-index, estimating BV^2
2. The *IDV*-index, estimating *B*
3. Polar Cap variation, estimating *VB*

These indices are readily computed from simple hourly means (or values) for which we have measurements stretching back into the early 19th Century. We can thus estimate the speed $V = \sqrt{[(BV^2) / B]}$ and use that value to calculate *VB* for comparison with the estimated *VB*, as shown in Figure 11. Although there are several second order effects, such as combined Rosenberg-Coleman and Russell-McPherron effects [e.g. Cliver et al., 2004], polar cap conductivity dependence on solar activity, and decrease of the geomagnetic dipole strength, that contribute to the small discrepancies found, the agreement is quite remarkable and strongly suggests that the determinations of *B* and *V* in the past are well in hand.

The Floor in the Heliospheric Magnetic Field

We can even do the analysis for a time scale of solar rotations, Figure 12. Note the 'floor' in *B* [Svalgaard & Cliver, 2007b; Owens et al., 2008]. A *B* floor implies the existence of a time-invariant component of the open solar flux, suggesting that the Heliospheric magnetic flux consists of a constant open flux component, with a time-varying contribution from the closed flux carried by coronal mass ejections (CMEs), which provides the solar cycle variation in *B*.

The return to the same value of *B* at each solar minimum means that flux added by CMEs must be balanced over the solar cycle, either by opening the closed flux via reconnection with open flux or by disconnecting an equivalent amount of open flux. The use of the treasure trove of hourly mean values has thus added important observational evidence to the modern discussion of Heliospheric magnetic field evolution; a point that would have delighted the early observers, as well as reminding *us* of the importance of preserving and digitizing the geomagnetic record.

Using the Dayside Data

It was known already to Rudolf Wolf in the 1850s that the amplitude of the diurnal variation of the Declination was a sensitive function of the sunspot number that he had just introduced [Wolf, 1859]. Figure 13(a) shows the clear difference between the variation of D at Praha (PRU) for sunspot maximum years (1957-1959) and sunspot minimum years (1964-1965). As Figure 13(b) shows, this variation was well observed even back in 1840-1849. Wolf used this relationship between the amplitude of the variation and the sunspot number as an aid in calibrating the sunspot number calculated from observations by other observers for times before his own observations started in 1849, and marveled: "Wer hätte noch vor wenigen Jahren an die Möglichkeit gedacht, aus den Sonnenflecken-beobachtungen ein terrestrisches Phänomen zu berechnen?"

The origin of these variations is the combined magnetic effects of ionospheric current vortices flowing in the E-region and of corresponding induced 'telluric' currents, created by dynamo action. Along the 'flanks' of the (external) vortices, the current flow is equatorwards on the morning side and polewards on the afternoon side. The magnetic effect at mid-latitudes of these currents at a right angle to the current flow is thus East-West. As the "ring current" and the auroral electrojets and their return currents that are responsible for geomagnetic activity have generally North-South directed magnetic effects (strongest at night), the daytime variation of the Y or East component is a suitable proxy for the strength of the S_R ionospheric current system.

The Declination can be converted to the East component using $Y = H \sin(D)$. The diurnal variation of Y is almost constant over a wide latitude range (20°-60°) and can readily be determined from hourly means. Using a large number of stations [Olso, Greenwich, Milan, Helsinki, Zi-Ka-Wei, etc] we can construct a composite series of the amplitude, rY, of the daily variation of Y from the 1840s until today, see Figure 14. The slight upwards trend is expected from the increase in ionospheric conductance due to the decrease of the geomagnetic dipole moment, and can be corrected for. The fact that the expected trend can even be detected attests to the accuracy of the determination of rY.

Calibrating the Sunspot Number

It is well-known that the strength of the S_R current system is a sensitive function of the conductance of the ionosphere which in turn can be well-described by the 10.7 cm solar radio flux. In fact, we can translate rY directly into an equivalent f10.7 flux as shown in Figure 15(a), and plot the flux calculated from the regression equation for comparison with the observed f10.7 radio flux in Figure 15(b).

Because the f10.7 radio flux depends on the sunspot number we can turn the calculated f10.7 flux into an equivalent sunspot number (Figure 16) and discover that there are indications that the calibration of even the venerable sunspot number before ~1945 is questionable. Both the Zürich and the Group Sunspot Number are too low before 1945 to account for the observed values of rY. The discrepancies correlate with Wolfer's change of sunspot counting method at Wolf's death in 1893 and the beginning of the inexperienced Waldmeier's tenure (1945) as the official keeper of the sunspot number.

The impersonal and objective determination of rY overcomes the subjective element in determination of the sunspot number and can safeguard its long-term calibration, as Wolf so rightly realized. The implications of a reassessment of the sunspot series are wide ranging. At the time of writing this is ongoing work. Space does not permit further elaboration here, but a preliminary report can be found in Svalgaard [2007].

Reconstruction of Total Solar Irradiance

As the sunspot number is often used as primary input to reconstructions of TSI, the Total Solar Irradiance, any re-calibration of the sunspot number series will impact TSI, and thus, through its use as a driver in climate models, the debate over climate change. Figure 17 shows a possible re-construction using a revised sunspot number series and compares it to several other current (and superseded – but still in use!) reconstructions. It is noteworthy that our reconstruction closely matches that of Preminger & Walton [2004] based on sunspot areas rather than sunspot numbers, and that the reconstructions over time have converged and now show a much smaller variation than initially thought, suggesting a much smaller impact on climate, unless the climate system is implausibly hypersensitive to changes in solar output.

Conclusions

1: The hourly values in yearbooks are an extremely valuable data source that allows us to calibrate our long-term geomagnetic and solar indices as far back as the geomagnetic record reaches.

2: By combinations of newly derived geomagnetic indices we can infer the physical properties of the solar wind in the past.

3. The availability of almost two centuries of reliable geomagnetic data has led to possible reassessments of several often-used indices of solar activity.

4: Every effort should be expended to preserve and digitize the treasure trove of 19th Century hourly data.

References

Cliver, E.W., L. Svalgaard, & A. G. Ling, Origins of the semiannual variation of geomagnetic activity in 1954 and 1996. *Annales Geophysicae*, ***22***(1), 93-100, 2004.

Emery, B. A., V. Coumans, D. S. Evans, G. A. Germany, M. S. Greer, E. Holeman, K. Kadinsky-Cade, F. J. Rich, & W. Xu, Seasonal, Kp, solar wind, and solar flux variations in long-term single-pass satellite estimates of electron and ion auroral hemispheric power, *Journal of Geophysical Research*, ***113***, A06311, doi:10.1029/2007JA012866, 2008.

Joos, G., J. Bartels, & P. Ten Bruggencate, Landolt-Börnstein: Zahlenwerte und Funktionen aus Physik, Chemie, Astronomie, Geophysik und Technik, Astronomie und Geophysik, XVIII, 795 pp., 331, Springer-Verlag, Berlin Heidelberg New York, 1952.

Jarvis, M. J., Observed tidal variation in the lower thermosphere through the 20th century and the possible implication of ozone depletion, *Journal of Geophysical Research*, ***110***, A04303, doi:10.1029/2004JA010921, 2005.

Karinen, A. & K. Mursula, A new reconstruction of the Dst index for 1932–2002, *Annales Geophysicae,* ***23***, 475–485, SRef-ID: 1432-0576/ag/2005-23-475, 2005.

Le Sager, P. & L. Svalgaard, No increase of the interplanetary electric field since 1926, *Journal of Geophysical Research*, ***109***, A07106, doi:10.1029/2004JA010411, 2004.

Love, J. J., Personal communication, 2007.

Mayaud, P. N., Calcul preliminaire d'indices Km, Kn et Ks ou Am, An, et As, mesures de l'activité magnétique a l'échelle mondiale et dans les hémispheres Nord et Sud, *Annales Geophysicae*, ***23***, 585, 1967.

Mayaud, P. N., The aa index: a 100-year series characterizing the geomagnetic activity, *Journal of Geophysical Research*, ***77***, 6870, 1972.

Mursula, K. & D. Martini, Centennial increase in geomagnetic activity: Latitudinal differences and global estimates, *Journal of Geophysical Research*, ***111***, A08209, doi:10.1029/2005JA011549, 2006.

O'Brien, T. P. & R. L. McPherron, Seasonal and diurnal variation of Dst dynamics, *Journal of Geophysical Research*, ***107***(A11), 1341, doi:10.1029/2002JA009435, 2002.

Owens, M. J., N. U. Crooker, N. A. Schwadron, T. S. Horbury, S. Yashiro, H. Xie, O. C. St. Cyr, & N. Gopalswamy, Conservation of open solar magnetic flux and the floor in the heliospheric magnetic field, *Geophysical Research Letters*, ***35***, L20108, doi:10.1029/2008GL035813, 2008.

Preminger, D. G. & S. R. Walton, Inferring Total and Spectral Solar Irradiance From Sunspot Areas Only, *American Geophysical Union*, Fall Meeting 2004, abstract #SH53A-0304, 2004.

Rouillard, A. P., M. Lockwood, & I. Finch, Centennial changes in the solar wind speed and in the open solar flux, *Journal of Geophysical Research*, ***112***, A05103, doi:10.1029/2006JA012130, 2007.

Svalgaard, L., Calibrating the Sunspot Number using 'the Magnetic Needle', (Climate And Weather of the Sun-Earth System) *CAWSES Newsletter*, ***4***, #1, http://www.bu.edu/cawses/calbrating_sunspot_number_using_mag_needle.pdf, 2007.

Svalgaard, L., E. W. Cliver, & A. G. Ling, The semiannual variation of great geomagnetic storms, *Geophysical Research Letters*, ***29***(16), 1765, doi:10.1029/2001GL014145, 2002.

Svalgaard, L., E. W. Cliver, & P. Le Sager, Determination of Interplanetary Magnetic Field Strength, Solar Wind Speed, and EUV Irradiance, 1890-Present, *International Solar Cycle Studies Symposium*, June 23-28, 2003, Tatranska Lomnica, Slovak Republic, Proceedings (ESA SP-535), 15, ed. A. Wilson. 2003.

Svalgaard, L., E. W. Cliver, & P. Le Sager, IHV: A new geomagnetic index, *Advances in Space Research*, ***34***(2), p.436-439, 2004.

Svalgaard, L. & E. W. Cliver, The IDV-Index: Its Derivation and Use in Inferring Long-term Variations of the Interplanetary Magnetic Field Strength, *Journal of Geophysical Research*, ***110***, A12103, doi:10.1029/2005JA011203, 2005.

Svalgaard, L. & E. W. Cliver, The InterHourly-Variability (IHV) Index of Geomagnetic Activity and its Use in Deriving the Long-term Variation of Solar Wind Speed, *Journal of Geophysical Research*, ***112***, A10111, doi:10.1029/2007JA012437, 2007a.

Svalgaard, L. & E. W. Cliver, A Floor in the Solar Wind Magnetic Field, *The Astrophysical Journal (Letters)*, ***661***, L203-L206, doi:10.1086/518786, 2007b.

Wolf, R., Schreiben des Herrn Prof. R. Wolf an den Herausgeber, Nr. 1185, *Astronomische Nachrichten*, ***50***, 141-144, 1859.

Several of the above papers, as well as related material, can be found at the author's website at http://www.leif.org/research

---

Figure Captions

Figure 1: Variation of the geomagnetic elements at Fredericksburg (FRD) over several days. Red boxes show local night. The first day (May 11, 1999) is the day when the solar wind famously 'disappeared'.

Figure 2: Monthly means of the InterHourly Variability index (*IHV*) for FRD [blue curve] and the *am*-index for the first 2 intervals of the UT-day [red curve]. The thin pink curve shows *IHV* scaled by 0.7475.

Figure 3: Stations used in the construction of the *IHV*-index. In 12 regions distributed in latitude and longitude *IHV* derived for the stations [red dots] are normalized to a reference station [pink]. *IHV* for an equatorial region [blue] is also calculated and found to match the mid-latitude regions. Stations above 55° corrected geomagnetic latitude are not to be used.

Figure 4: (a) A section of Bartels 27-day rotation averages of the *IHV*-index showing all Northern Hemisphere [black] and Southern Hemisphere [red] regional *IHV*s. (b) The composite *IHV*-index for each rotation since 1883 [grey] and the 13-rotation running mean [heavy black].

Figure 5: Observed [red] and calculated (from regression equations) [blue] 27-day rotation averages (top) of *Am*-index, (middle) of *Ap*-index, (bottom) of *Aa*-index.. Heavier curves show 13-rotation running means. All indices have been freed from the equinoctial effect using eq.(1).

Figure 6: Synthetic individual *am* 3-hour values calculated [red] from solar wind parameters using eq.(2) and corresponding observed *am* values for six Bartels rotations. The scale is logarithmic to show how well calculated and observed values match at all scales. The match is poor for *am* < 5 nT where the index is very difficult to measure or where the coupling function is less valid.

Figure 7: (a) Correlation of all rotation means of *IHV* with BV_o^2 (where V_o is a shorthand for V in units of 100 km/s) as observed by spacecraft. (b) Detailed comparison of observed and calculated [using the regression equation above] BV_o^2 for a twelve year interval, 1980-1992.

Figure 8: Yearly average *u*-measures in 1 nT units [blue] and *IDV*-index values [red].

Figure 9: (a) Correlations between yearly values of *B* and *V* versus *IDV*. It is clear that there is a robust (R^2 = 0.88) correlation with *B*, but none with *V*. (b) Runs of *V*, *B*, and *IDV* since the beginning of the spacecraft era. Lack of matching response to *V* is shown by dark arrows, while matching responses to *B* are shown by pink arrows. The failure of the *u*-measure to record the recurrent high-speed streams in 1930 now becomes clear.

Figure 10: (a) The average variation [over 1980-2004] of the end point of the vector from hour to hour (symbols) of the magnetic effect of the overhead current sheet for ALE (Alert), THL (Thule), RES (Resolute Bay), CBB (Cambridge Bay), and BLC (Baker Lake). Whenever a station is inside the polar cap it feels the effect of the uniform current seen by all. (b) Similar vector diagram for Kingua-Fjord during the first Polar Year1882-1883 http://www.arctic.noaa.gov/aro/ipy-1/Series-NB-P1.htm .

Figure 11: (a) Yearly values of *B* deduced from *IDV* and of V_o deduced from *IHV* (with *B* from *IDV*), blue curves, compared to spacecraft values, red curves. (b) BV_o (blue curve) computed from *B* and V_o taken from (a) compared to BV_o computed using spacecraft data (red curve) and deduced from polar cap diurnal vector 'circle' variation [c.f. Figure 10] (green curve).

Figure 12: (a) Bartels rotation average *B* deduced from *IDV* (black) and measured by spacecraft (red). Note the 'floor'. The green line is a 4th order polynomial fit to indicate an approximate smooth trend. Heavy curves show 13-rotation running means. (b) Same, but for V_o.

Figure 13: (a) Diurnal and seasonal variation of the Declination at Praha (PRU). For each month the graph shows the local time variation (blue curves) and for the whole year (red). Sunspot maximum [1957-1959] is shown by darker colored curves, while sunspot minimum [1964-1965] is shown by lighter colored curves. (b) Same, but for the interval 1840-1849. The definition of the full range, *rY*, is shown by the arrow.

Figure 14: The variation since 1841 of *rY* derived from several stations as described in the text. The solar cycle effect is clearly seen. The minimum values (when no spots are present) show a slight increasing trend consistent with the increase of ionospheric conductance due to the declining geomagnetic dipole moment. Removing the trend results in the red curve.

Figure 15: (a) Correlation between yearly averages of f10.7 radio flux and the diurnal range, *rY*, over the interval 1947-2005. (b) Comparison of observed f10.7 radio flux (red) and flux calculated from the above regression equation (blue).

Figure 16: Calculated (blue curve) yearly average International Sunspot Number, R_I, from *rY* since 1841. Observed yearly averages of R_I, or R_Z (red) and Group Sunspot Number, R_G, (gray) are shown for comparison. Each cycle is marked with the number of the cycle. Note the overlap between panels.

Figure 17: Several reconstruction of TSI (Total Solar Irradiance) from 1993 [Hoyt & Schatten] onwards. There is a progressive decrease with time of publication of the amplitude of the estimated variation. Modern reconstructions keep the variation of TSI within about 1 W/m^2.

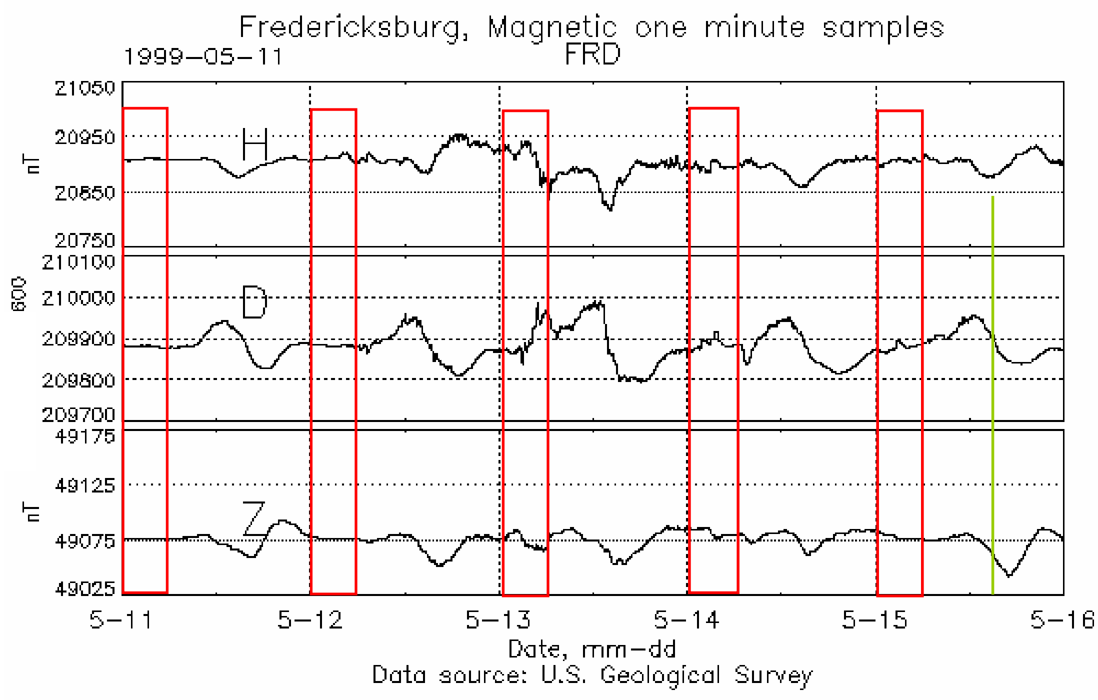
Fredericksburg, Magnetic one minute samples
1999-05-11
FRD
21050
20950
20850
20750
nT
H
210100
210000
209900
209800
209700
600
D
49175
49125
49075
49025
nT
Z
5-11
5-12
5-13
5-14
5-15
5-16
Date, mm-dd
Data source: U.S. Geological Survey

Figure 1

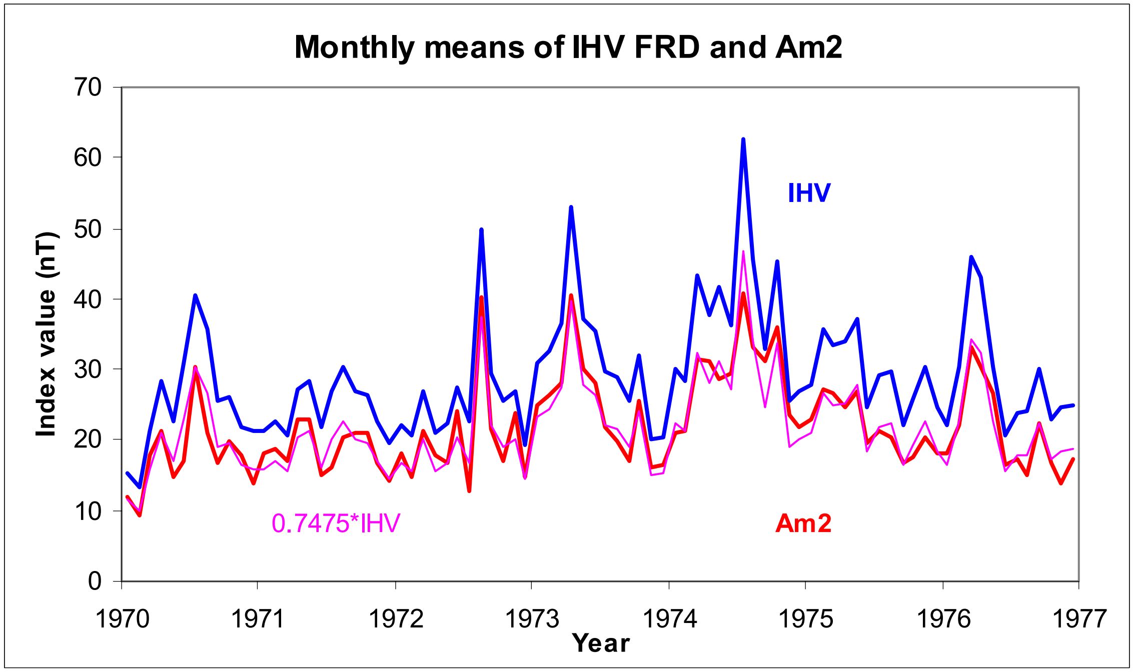

Monthly means of IHV FRD and Am2
Index value (nT)
70
60
50
40
30
20
10
0
1970
1971
1972
1973
1974
1975
1976
1977
Year
IHV
0.7475*IHV
Am2

Figure 2

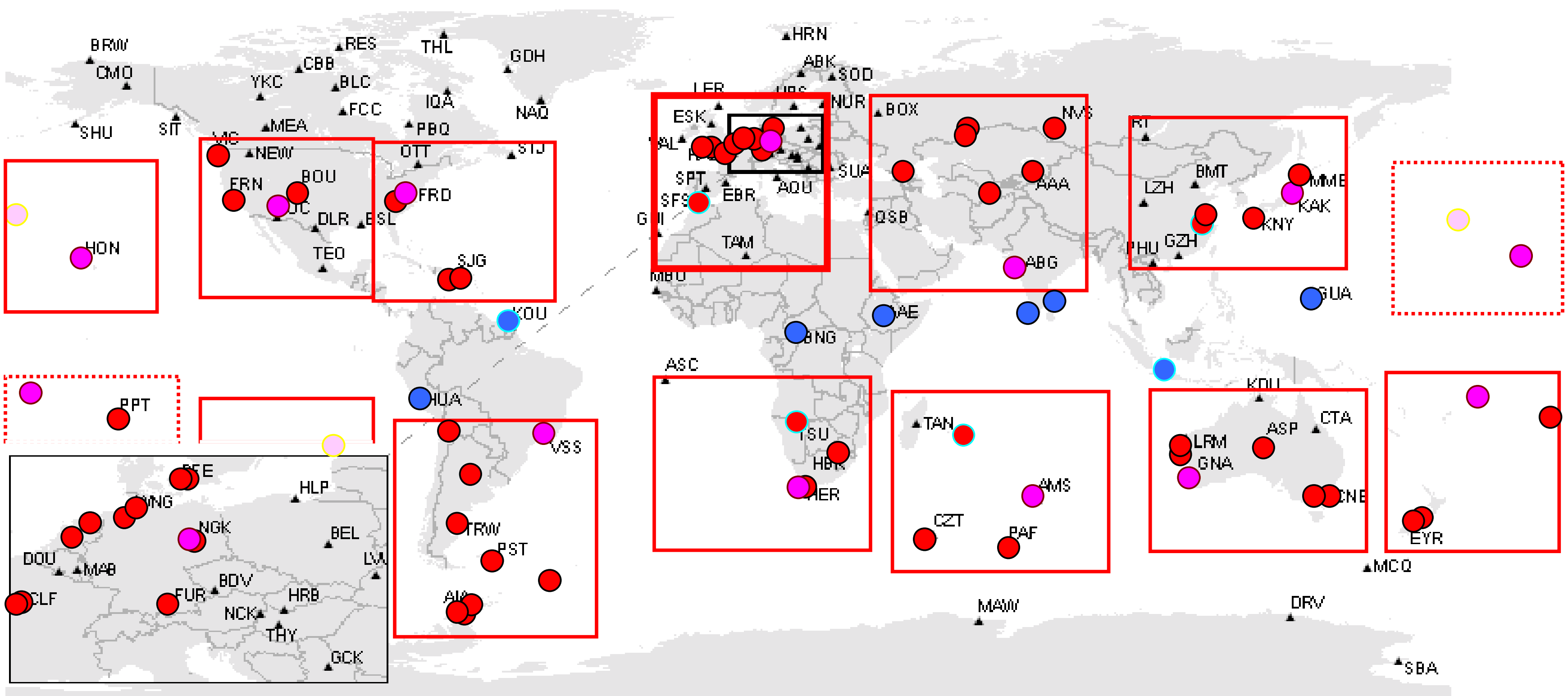
BRW
CMO
SHU
SIT
YKC
CBB
RES
BLC
FCC
MEA
THL
IQA
PBQ
GDH
NAQ
NEW
FRN
BOU
DLR
BSL
TEO
OTT
STJ
FRD
SJG
HON
PPT
KOU
HUA
VSS
TRW
PST
HLP
BEL
NGK
DOU
MAB
CLF
FUR
BDV
HRB
NCK
THY
GCK
HRN
ABK
SOD
NUR
LER
ESK
SPT
SFS
EBR
AQU
SUA
TAM
MBO
ASC
BNG
AAE
BOX
QSB
NVS
AAA
ABG
TSU
HBK
HER
TAN
AMS
CZT
PAF
MAW
LZH
BMT
MMB
KAK
KNY
GZH
PHU
GUA
KDU
ASP
CTA
LRM
GNA
CNB
EYR
MCQ
DRV
SBA

Figure 3

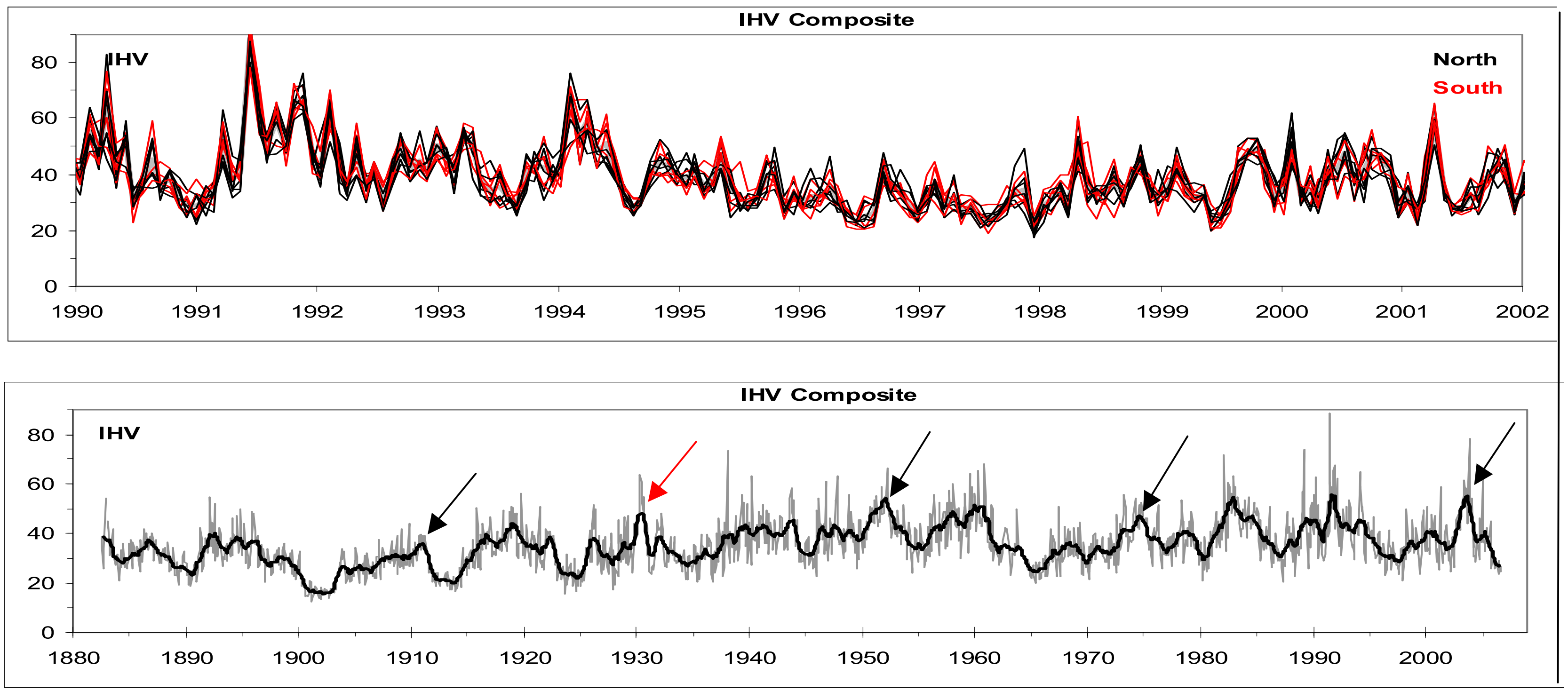
IHV Composite
IHV
North
South
80
60
40
20
0
1990
1991
1992
1993
1994
1995
1996
1997
1998
1999
2000
2001
2002
IHV Composite
IHV
80
60
40
20
0
1880
1890
1900
1910
1920
1930
1940
1950
1960
1970
1980
1990
2000

Figure 4

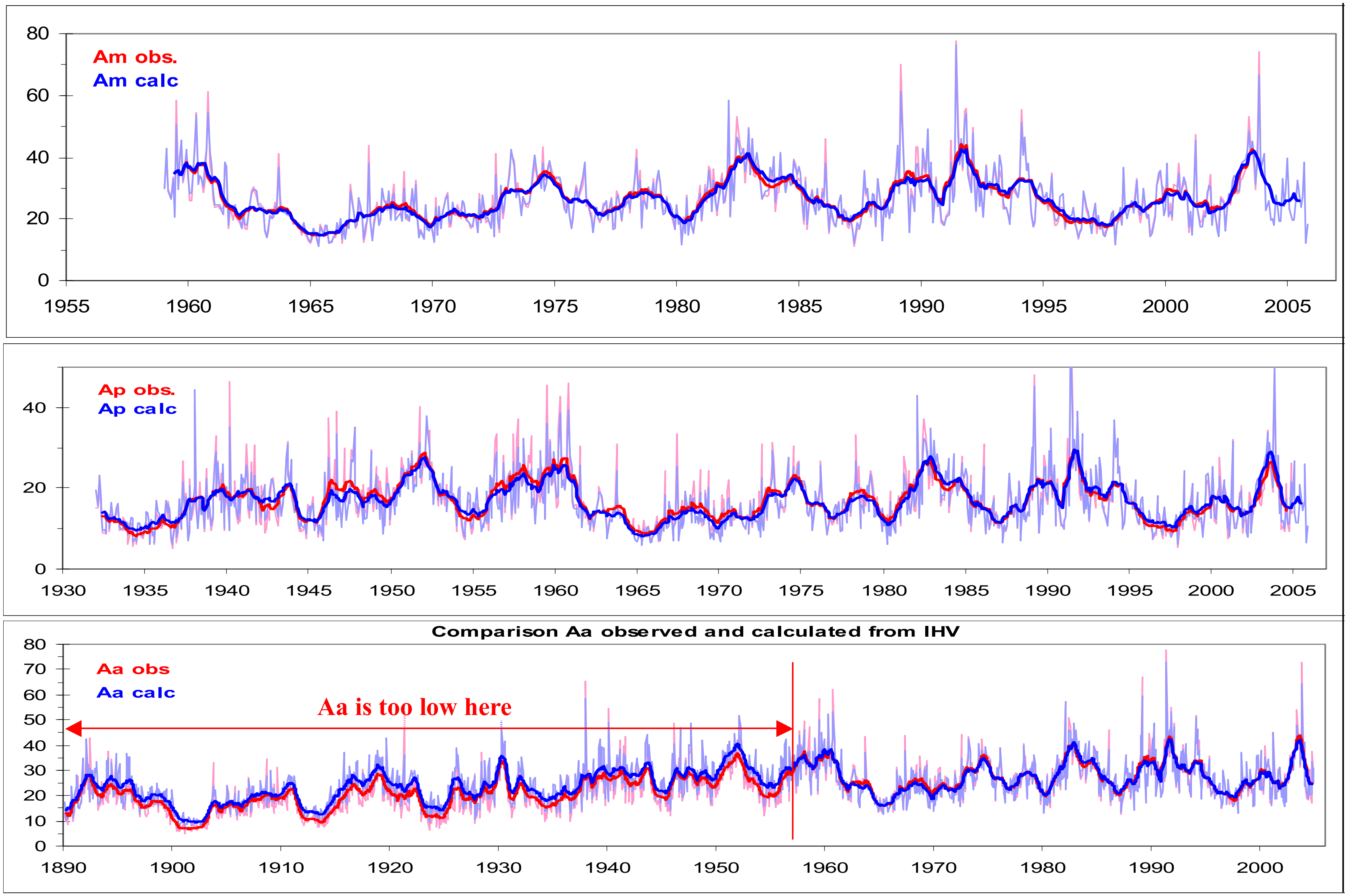
Am obs.
Am calc
Ap obs.
Ap calc
Comparison Aa observed and calculated from IHV
Aa obs
Aa calc
Aa is too low here

Figure 5

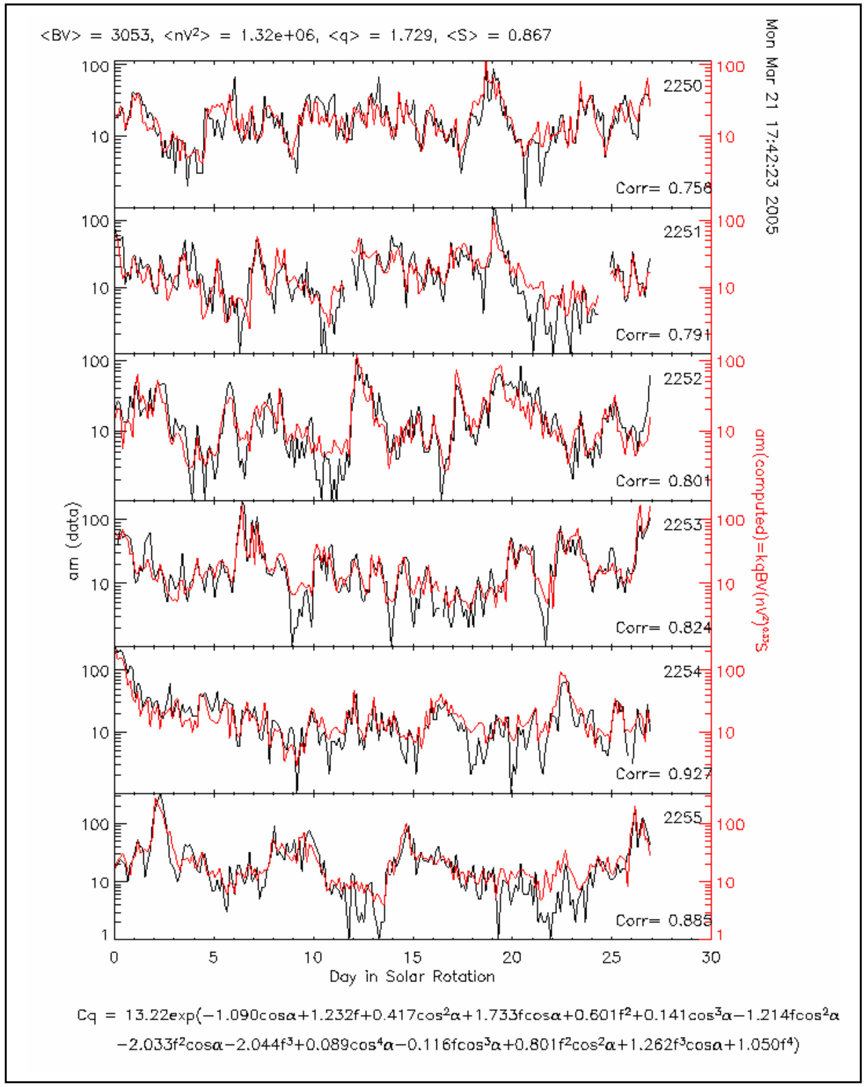

<BV> = 3053, <nV²> = 1.32e+06, <q> = 1.729, <S> = 0.867
Mon Mar 21 17:42:23 2005
am (data)
am(computed)=kqBV(nV²)^0.33 S
2250
Corr= 0.758
2251
Corr= 0.791
2252
Corr= 0.801
2253
Corr= 0.824
2254
Corr= 0.927
2255
Corr= 0.885
Day in Solar Rotation
Cq = 13.22exp(−1.090cosα+1.232f+0.417cos²α+1.733fcosα+0.601f²+0.141cos³α−1.214fcos²α
−2.033f²cosα−2.044f³+0.089cos⁴α−0.116fcos³α+0.801f²cos²α+1.262f³cosα+1.050f⁴)

Figure 6

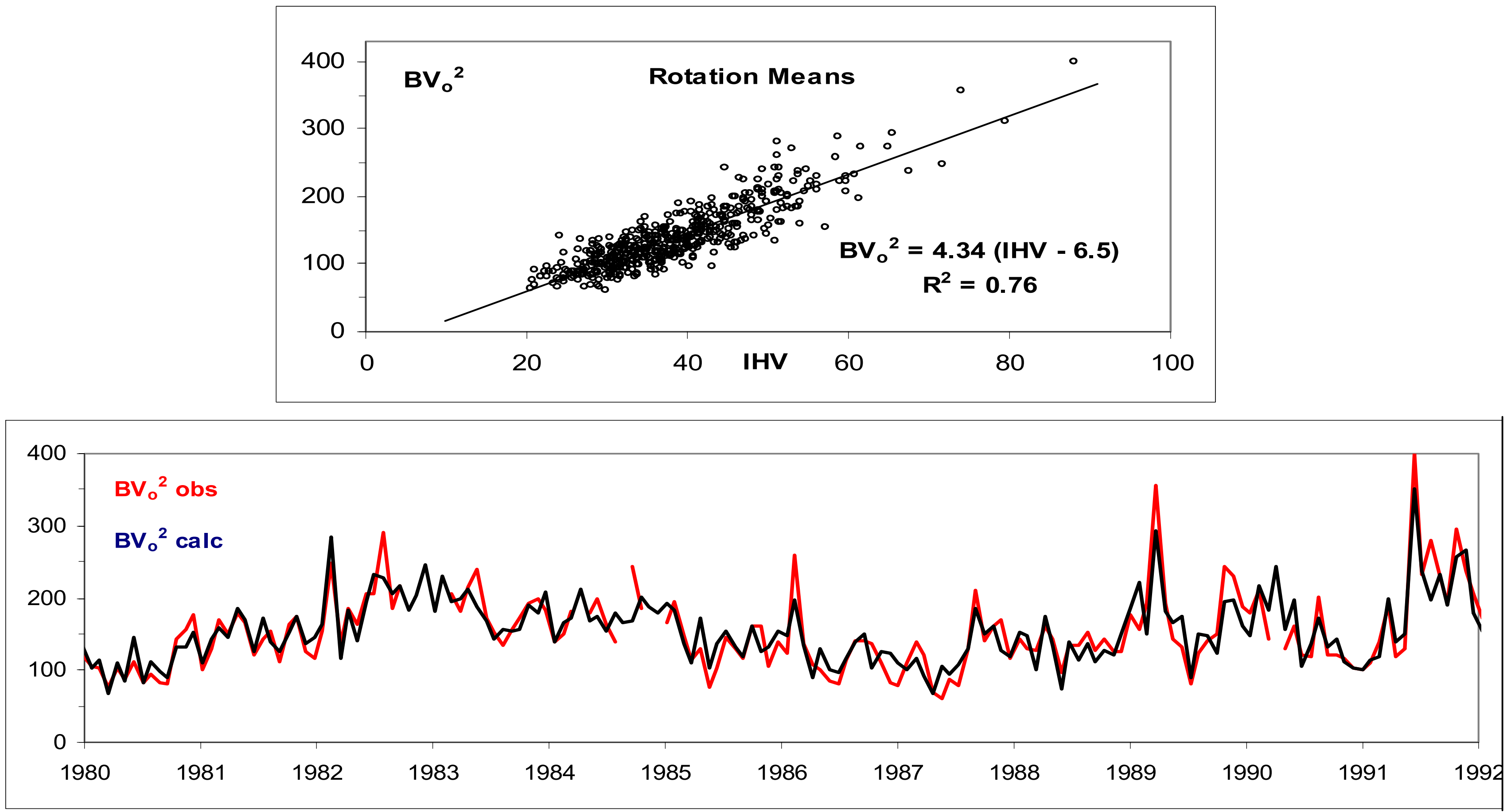

Rotation Means
BV_o^2
$BV_o^2 = 4.34\ (IHV - 6.5)$
$R^2 = 0.76$
IHV
0
20
40
60
80
100
0
100
200
300
400
BV_o^2 obs
BV_o^2 calc
1980
1981
1982
1983
1984
1985
1986
1987
1988
1989
1990
1991
1992

Figure 7

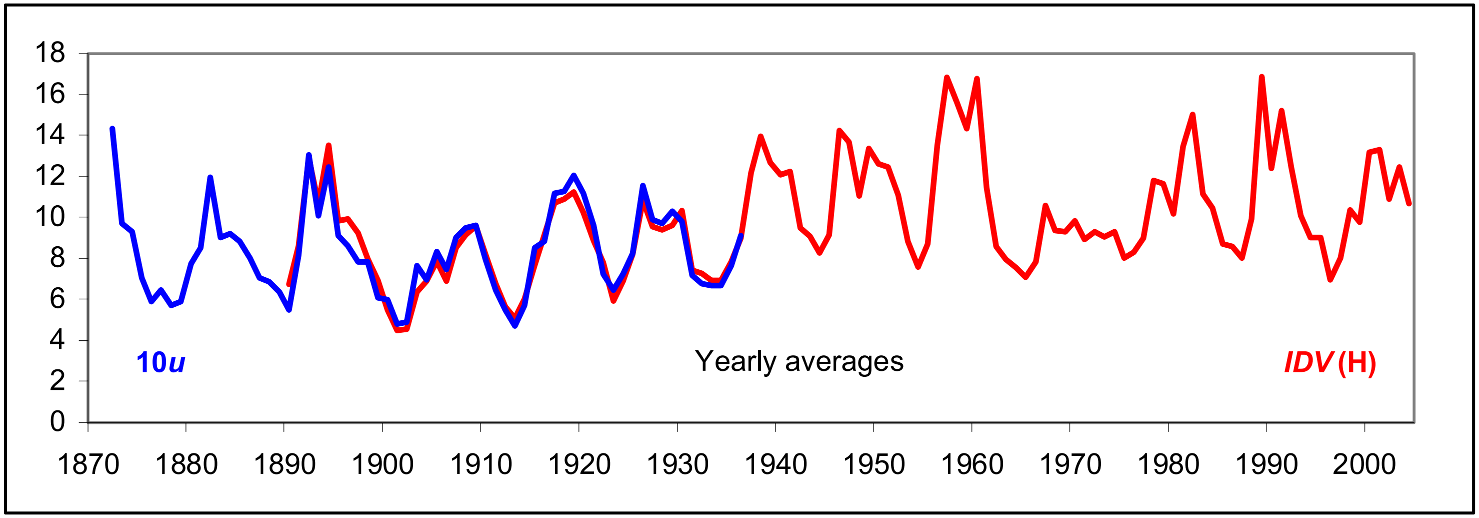
18
16
14
12
10
8
6
4
2
0
10u
Yearly averages
IDV (H)
1870
1880
1890
1900
1910
1920
1930
1940
1950
1960
1970
1980
1990
2000

Figure 8

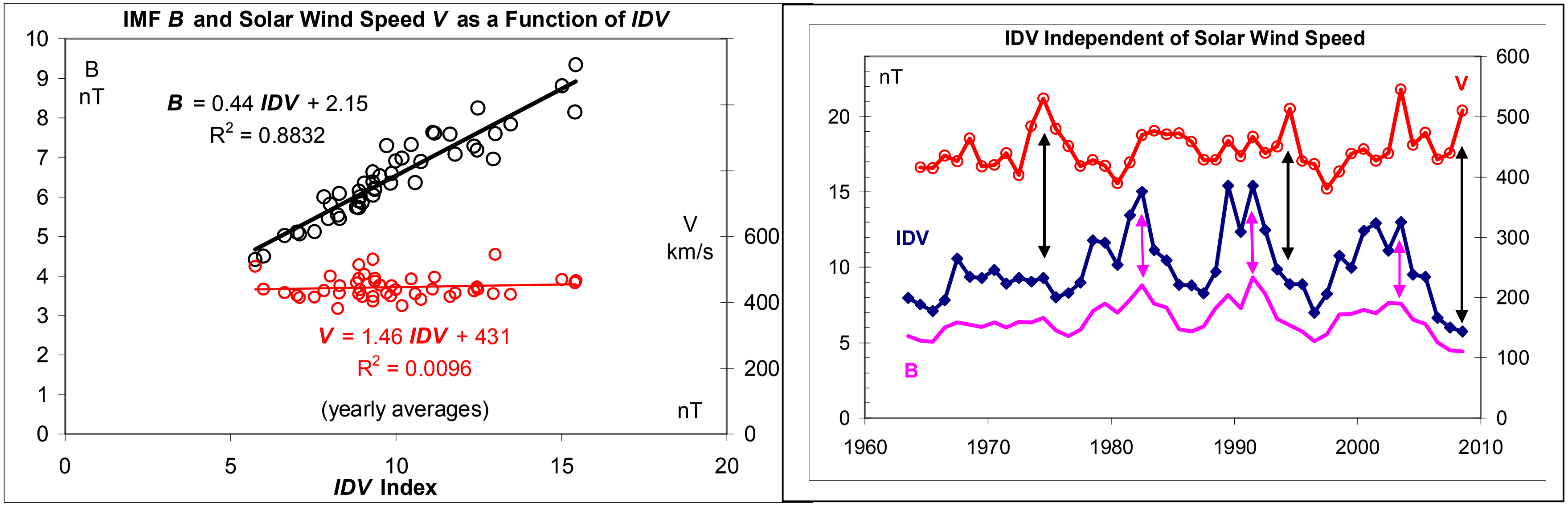
IMF B and Solar Wind Speed V as a Function of IDV
B
nT
B = 0.44 IDV + 2.15
R2 = 0.8832
V
km/s
V = 1.46 IDV + 431
R2 = 0.0096
(yearly averages)
nT
IDV Index
IDV Independent of Solar Wind Speed
nT
V
IDV
B

Figure 9

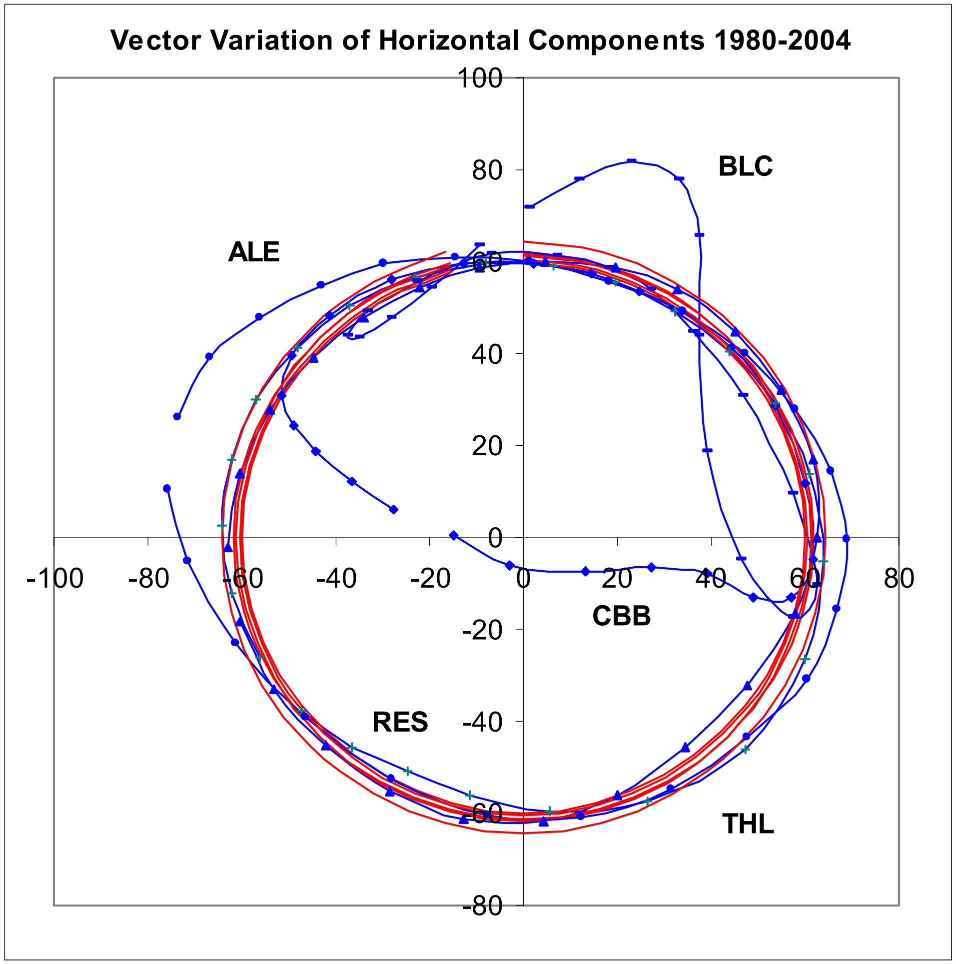

Vector Variation of Horizontal Components 1980-2004
ALE
BLC
CBB
RES
THL
100
80
60
40
20
0
-20
-40
-60
-80
-100

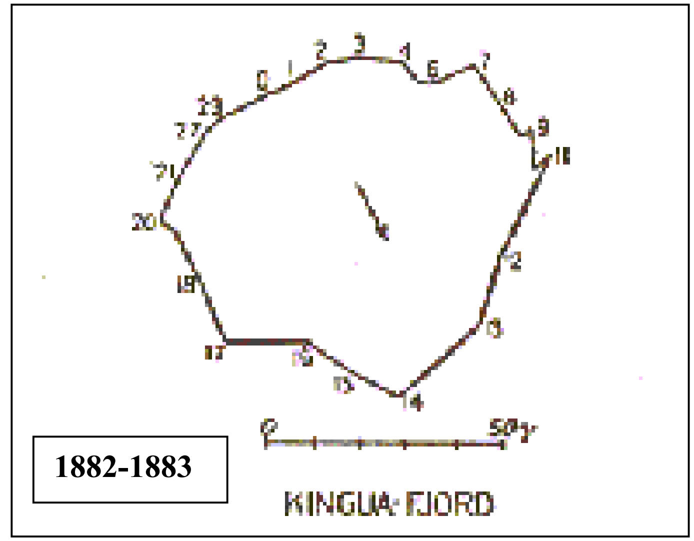

1882-1883
KINGUA FJORD

Figure 10

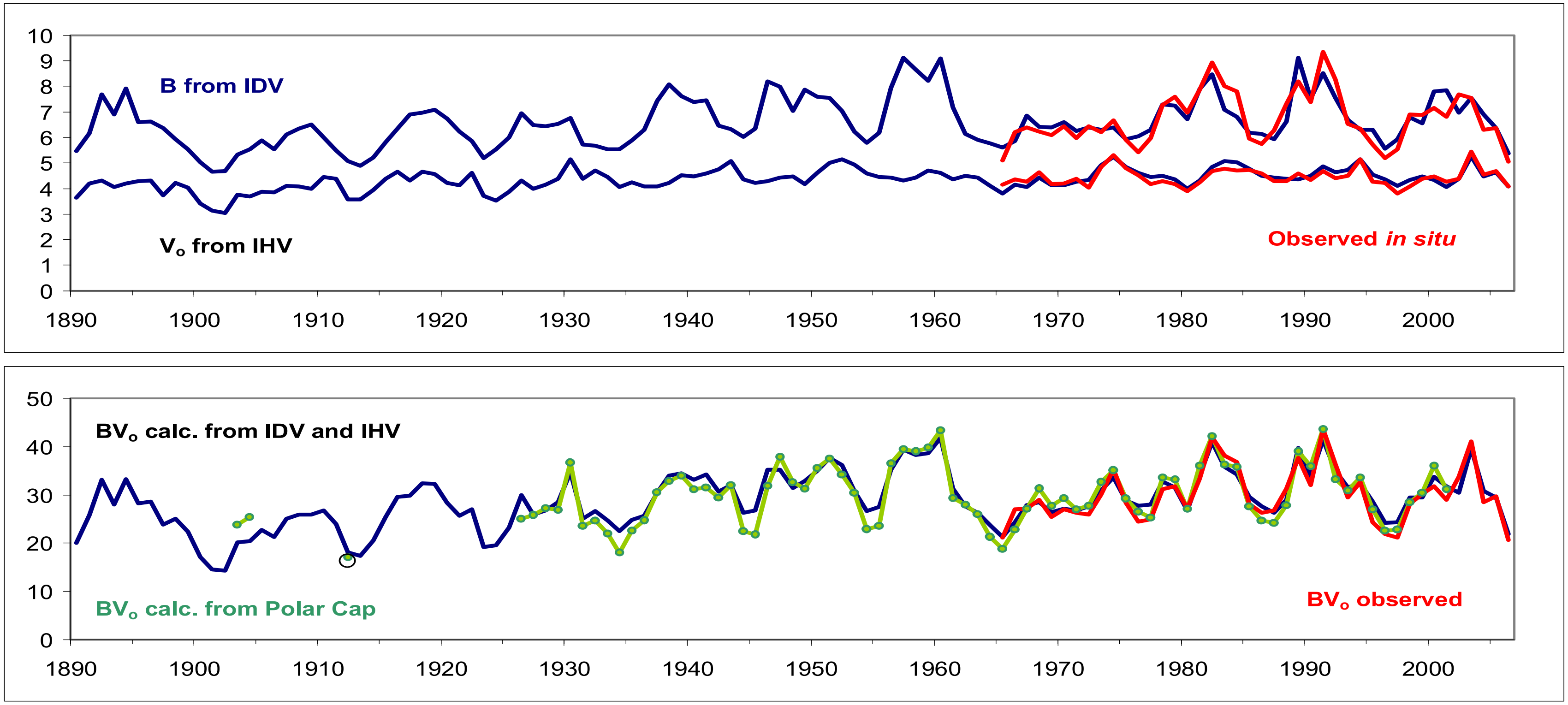
B from IDV
V$_o$ from IHV
Observed *in situ*
BV$_o$ calc. from IDV and IHV
BV$_o$ calc. from Polar Cap
BV$_o$ observed

Figure 11

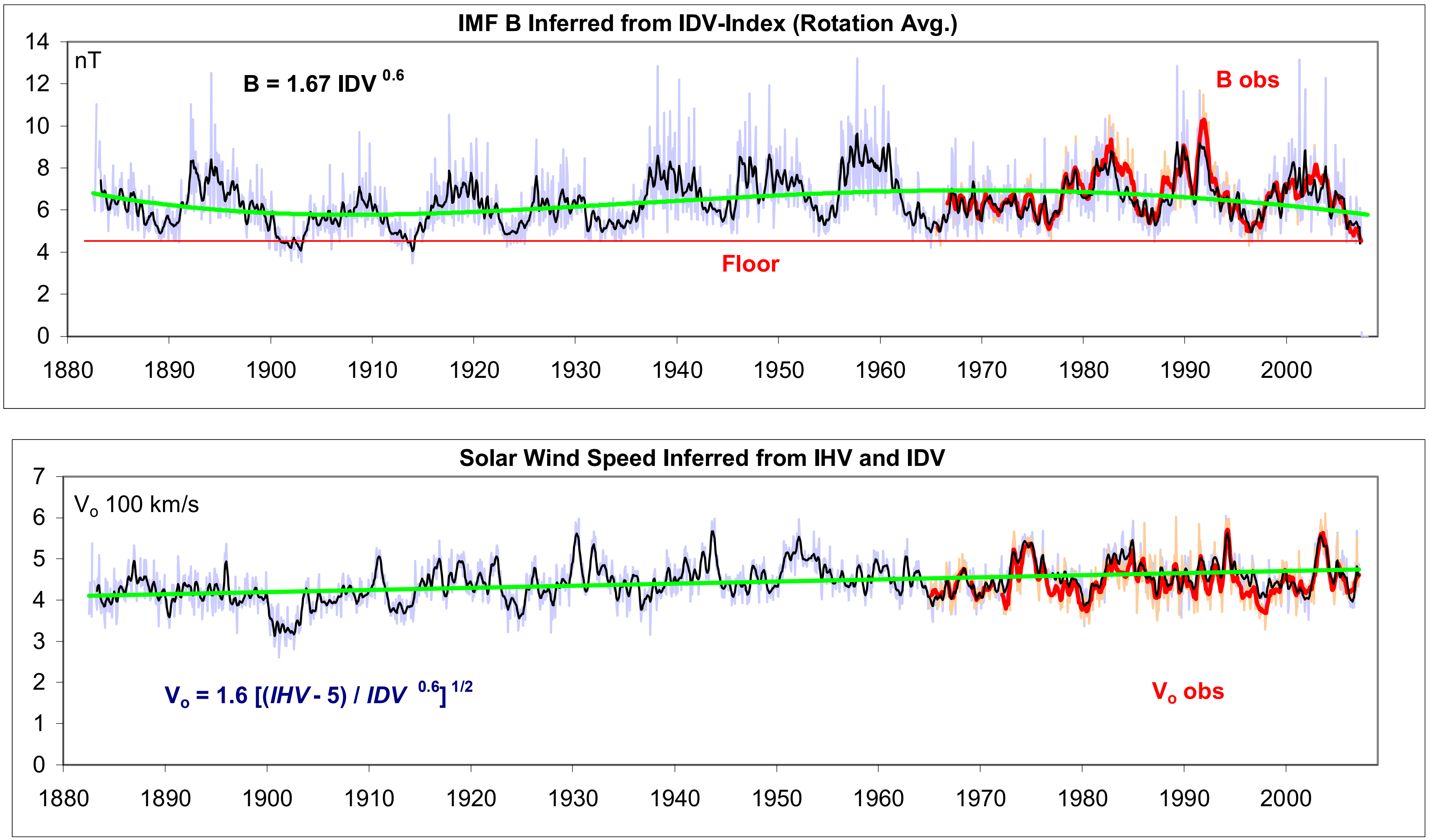

IMF B Inferred from IDV-Index (Rotation Avg.)
nT
B = 1.67 IDV 0.6
B obs
Floor
14
12
10
8
6
4
2
0
1880
1890
1900
1910
1920
1930
1940
1950
1960
1970
1980
1990
2000
Solar Wind Speed Inferred from IHV and IDV
Vo 100 km/s
Vo = 1.6 [(IHV - 5) / IDV 0.6] 1/2
Vo obs
7
6
5
4
3
2
1
0
1880
1890
1900
1910
1920
1930
1940
1950
1960
1970
1980
1990
2000

Figure 12

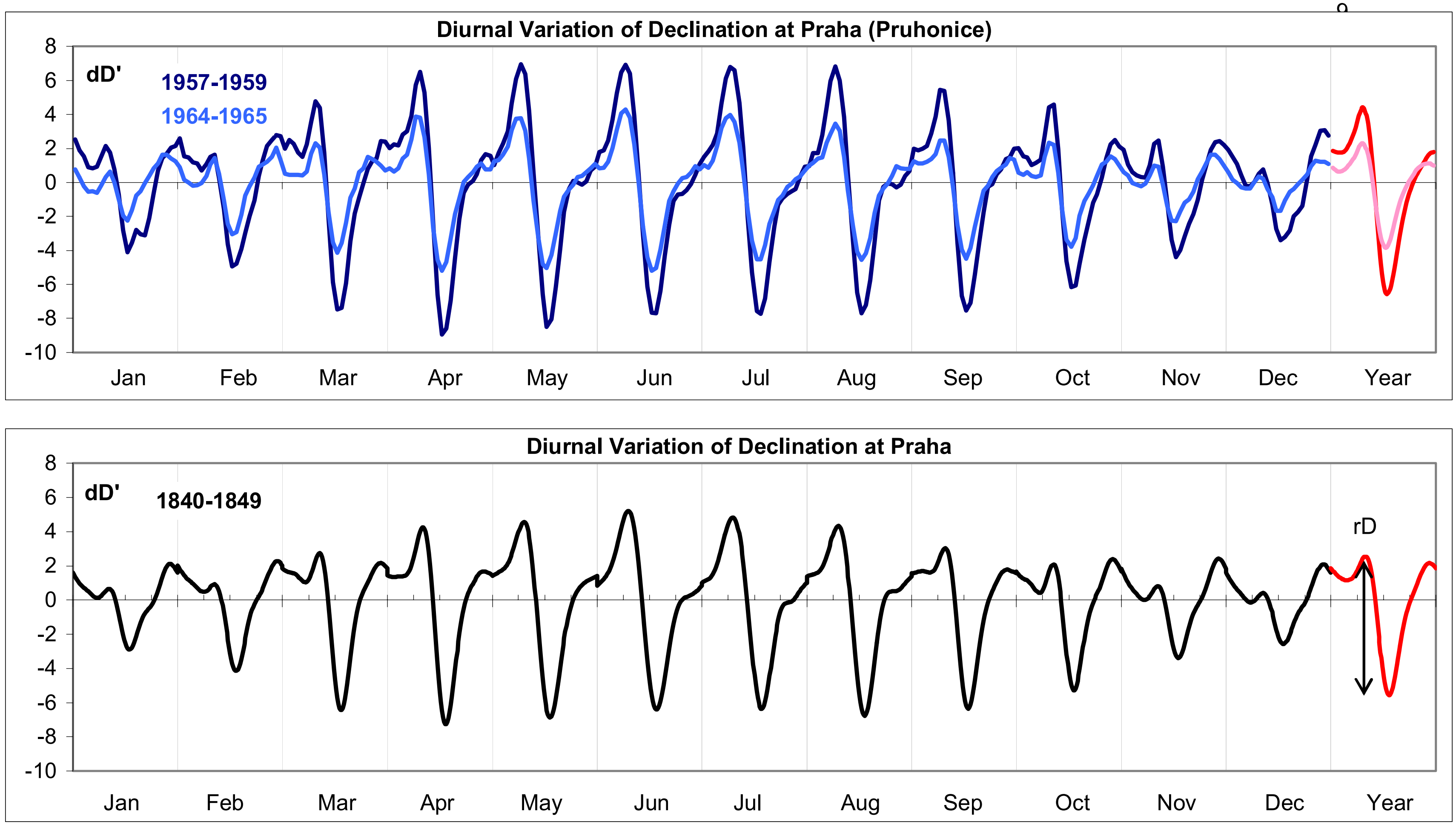
Diurnal Variation of Declination at Praha (Pruhonice)
dD'
1957-1959
1964-1965
8
6
4
2
0
-2
-4
-6
-8
-10
Jan
Feb
Mar
Apr
May
Jun
Jul
Aug
Sep
Oct
Nov
Dec
Year
Diurnal Variation of Declination at Praha
dD'
1840-1849
rD
8
6
4
2
0
-2
-4
-6
-8
-10
Jan
Feb
Mar
Apr
May
Jun
Jul
Aug
Sep
Oct
Nov
Dec
Year

Figure 13

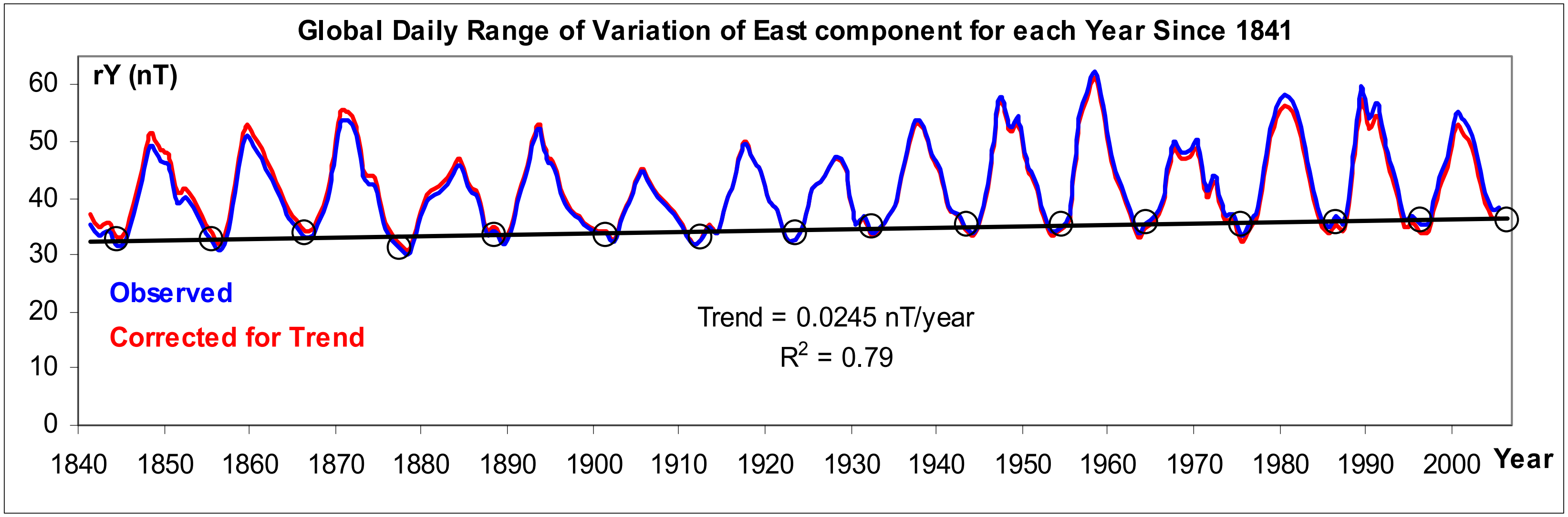
Global Daily Range of Variation of East component for each Year Since 1841
rY (nT)
60
50
40
30
20
10
0
1840
1850
1860
1870
1880
1890
1900
1910
1920
1930
1940
1950
1960
1970
1980
1990
2000
Year
Observed
Corrected for Trend
Trend = 0.0245 nT/year
R2 = 0.79

Figure 14

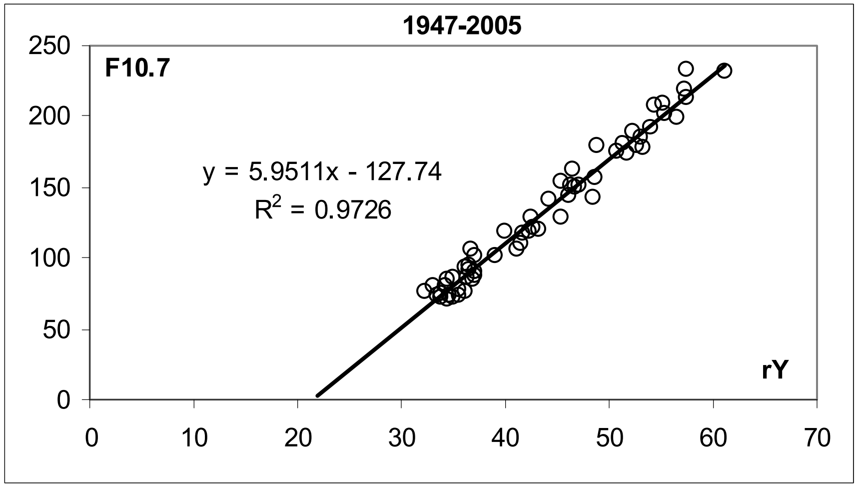
1947-2005
F10.7
y = 5.9511x - 127.74
R2 = 0.9726
rY
250
200
150
100
50
0
0
10
20
30
40
50
60
70

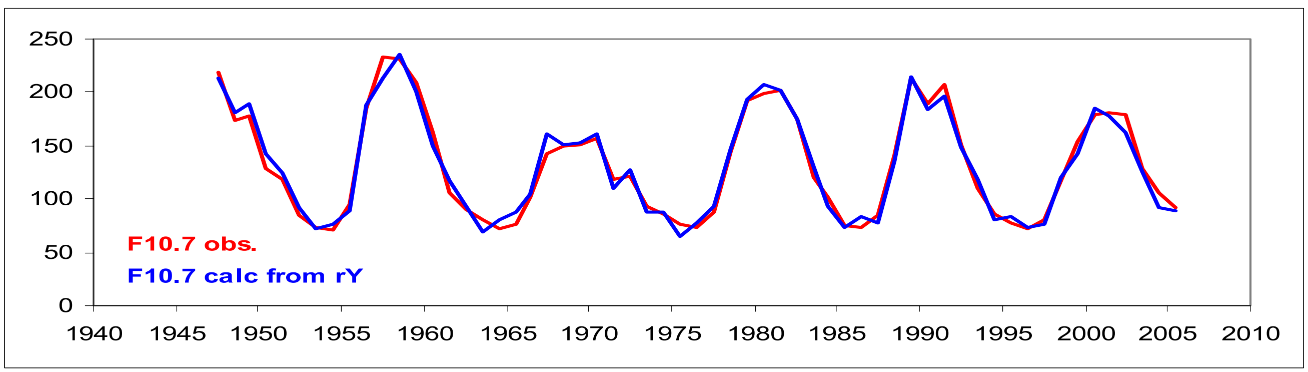
F10.7 obs.
F10.7 calc from rY
250
200
150
100
50
0
1940
1945
1950
1955
1960
1965
1970
1975
1980
1985
1990
1995
2000
2005
2010

Figure 15

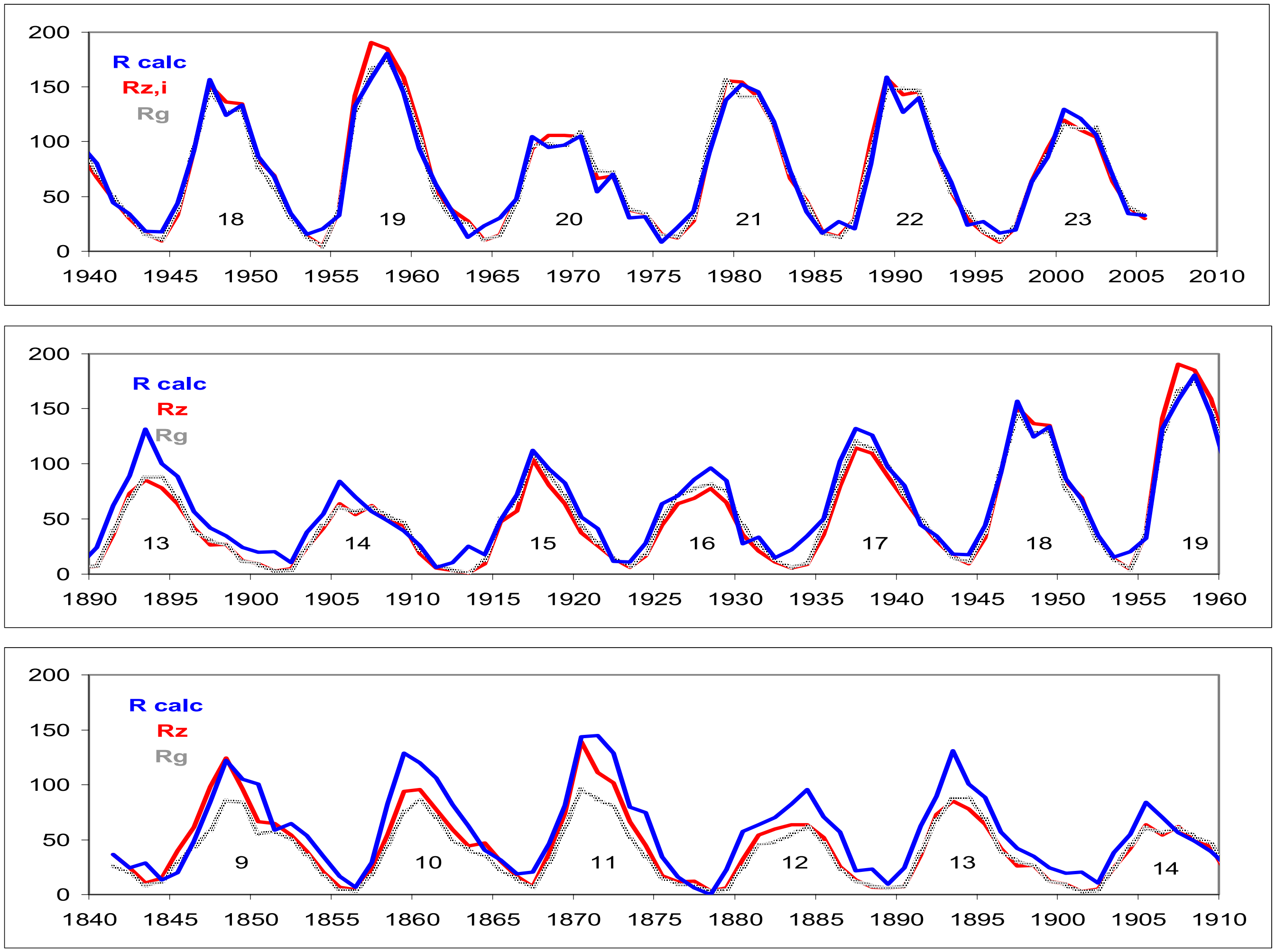

Figure 16

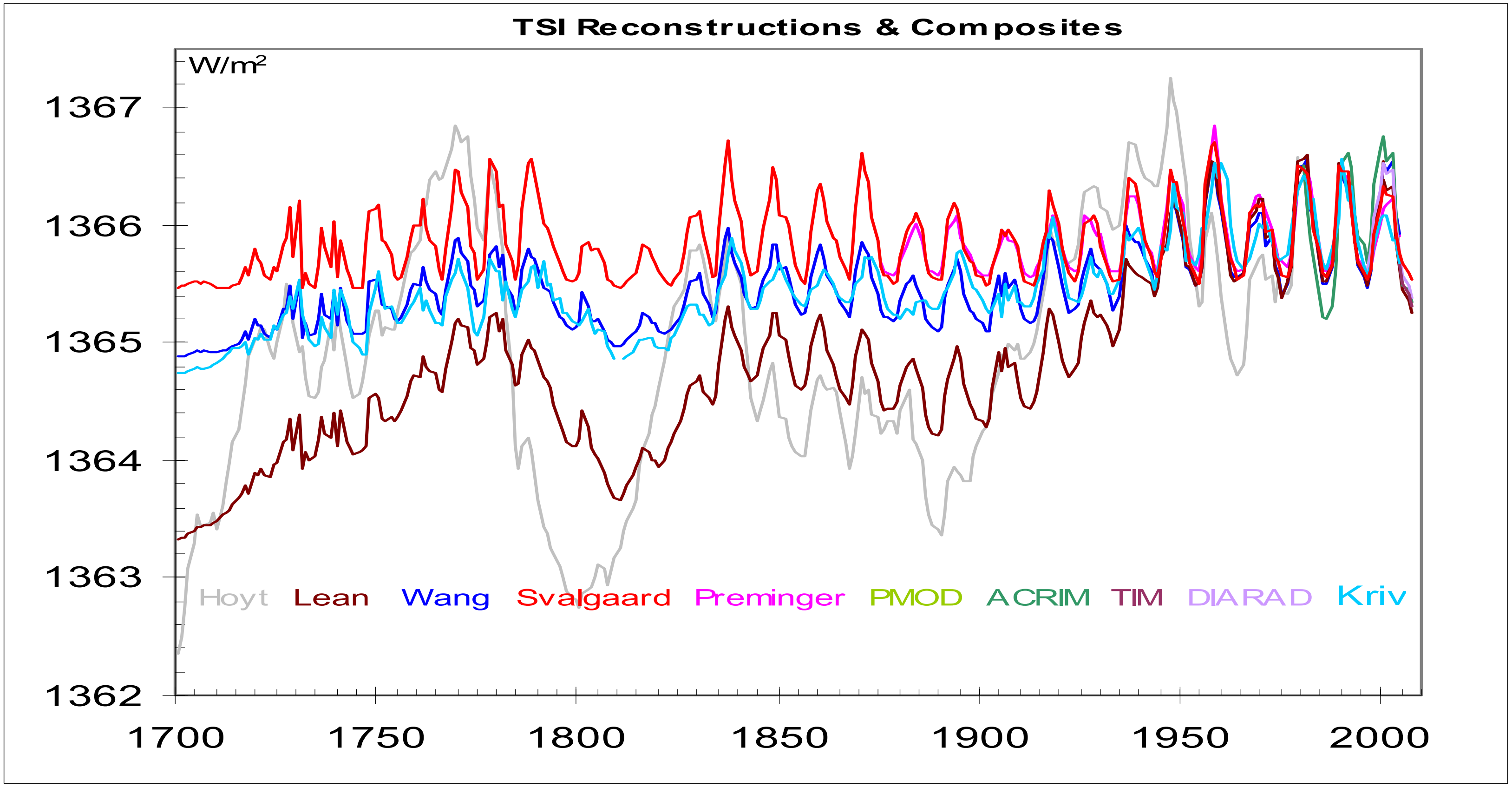
TSI Reconstructions & Composites
W/m²
1367
1366
1365
1364
1363
1362
1700
1750
1800
1850
1900
1950
2000
Hoyt
Lean
Wang
Svalgaard
Preminger
PMOD
ACRIM
TIM
DIARAD
Kriv

Figure 17